Mineralogical Magazine, April 2017, Vol. 81(2), pp. 355–368

The crystal structure of veenite

DAN TOPA[1,*] AND EMIL MAKOVICKY[2]

[1] Natural History Museum Vienna, Burgring 7, 1010 Vienna, Austria
[2] Institute for Geoscience and Mineral Resources Management, University of Copenhagen, Østervoldgade 10, DK-1350, Copenhagen K, Denmark

[*Received 24 November 2015; Accepted 30 July 2016; Associate Editor: Ed Grew*]

ABSTRACT

The crystal structure of veenite is reported for the first time from a sample from the type locality of Madoc (Ontario, Canada). It has been solved and refined by X-ray single-crystal diffraction on the basis of 4973 observed reflections (with $F_o > 4\sigma(F_o)$) with a final $R_1 = 0.0396$. Veenite is monoclinic $P2_1$, with unit-cell parameters $a = 8.429(2)$, $b = 26.069(5)$, $c = 8.962(2)$ Å, $\beta = 117.447(2)^o$. The bulk veenite composition is $Ag_{0.15}Pb_{16.029}Sb_{8.836}As_{6.99}S_{39.95}$ (for $Z = 1$) corresponding to N = 4.09 ($Me_{8N}S_{8N+8}$, theoretical value is 4.0), with the percentage of the Ag-(As,Sb) substituted end-member only equal to 3.51 mol.%, i.e., a nearly pure Pb-Sb-As sulfosalt. The crystal structure is typical for the N = 4 sartorite homologue, with zig-zag walls of trigonal coordination prisms of Pb which separate slabs of diagonally oriented double-layers populated by Sb and As with partial Pb substitution. Orientation of three-membered crankshaft chains formed by strong (As,Sb) – S bonds on the two surfaces of double-layers differs substantially from that in dufrénoysite, which is a pure Pb-As (N = 4) sulfosalt.

KEYWORDS: veenite, single-crystal structure, dufrénoysite, sartorite homologous series, Madoc, Canada.

Introduction

VEENITE was described by Jambor (1967) who defined it as $Pb_2(Sb,As)_2S_5$, with an orthorhombic subcell (space group $P2_1cn$ or *Pmcn)*, with $a = 4.22$ Å, $b = 26.2$ Å and $c = 7.90$ Å. According to Jambor (1967), the true structure has a doubled a parameter, 8.44 Å and unknown symmetry. Veenite appeared to form twin lamellae when observed in reflected light. The type locality is Madoc, Ontario, Canada. Veenite is the N = 4 member of the sartorite homologous series of Pb-As-Sb sulfosalts. The mineral was defined as an Sb-containing analogue of dufrénoysite, $Pb_2As_2S_5$, which was described originally from the antimony-poor locality of Lengenbach, Switzerland. In the original veenite, the Sb:As ratio was close to 5:3 = 1.67. The present contribution reports a detailed restudy of chemistry and crystal structure of veenite based on the material (sample M53762) from the original locality, kindly supplied by Drs. Kim Tait and Brendt Hyde, and preserved at the Royal Ontario Museum, Toronto, Canada.

Chemical data

New electron microprobe analyses, obtained on the association of veenite, sterryite, bournonite, boulangerite and geocronite, were performed using a JEOL Hyperprobe JXA-8530F electron microprobe (installed at Natural History Museum, Vienna, Austria) operated at 25 kV and 20 nA, with a beam diameter of 2 μm. Wavelength-dispersive spectroscopic data were collected using the following standards and emission lines: galena (Pb$M\alpha$), chalcopyrite (Cu$K\alpha$), Ag metal (Ag$L\alpha$), stibnite (Sb$L\alpha$) and lorandite (As$L\alpha$, S$K\alpha$). No other elements were detected. The raw data were corrected for matrix effects with the JEOL on-line *ZAF* procedure including a correction for partial overlapping of As$L\alpha$ with Sb$L\alpha$ ($n = 3$) lines. The results of the electron-microprobe analyses for veenite and associated minerals are compiled in

*E-mail: dan.topa@nhm-wien.ac.at
https://doi.org/10.1180/minmag.2016.080.141

© 2017 The Mineralogical Society

https://doi.org/10.1180/minmag.2016.080.141 Published online by Cambridge University Press

https://doi.org/10.1180/minmag.2016.080.141 Published online by Cambridge University Press

TABLE 1. Electron microprobe chemical data of veenite and associated minerals.

No.	NA*	Mineral	BSE	Cu	Ag	Pb	Sb	As	S	Total	ch[#]	$N^{\S}_{calc}$
[1]	102	veenite	medium[$]	n.d.	0.18(08)	53.48(47)	17.25(30)	8.41(28)	20.55(12)	99.87(35)	−0.1	4.08
[2]	7	veenite	dark	n.d.	0.16(09)	53.31(50)	16.58(11)	9.05(17)	20.69(15)	99.80(22)	−0.3	4.04
[3]	10	veenite	bright	n.d.	0.16(06)	53.31(27)	17.61(08)	8.23(08)	20.50(06)	99.81(33)	0.1	4.07
[4]	23	sterryite	medium	0.78(09)	3.34(17)	46.82(45)	21.08(46)	7.19(23)	20.65(14)	99.85(35)	1.3	–
[5]	6	sterryite	dark	0.90(11)	3.23(22)	46.61(35)	21.56(39)	6.86(16)	20.56(09)	99.71(13)	1.5	–
[6]	17	sterryite	bright	0.74(02)	3.38(12)	46.90(46)	20.91(35)	7.30(10)	20.68(15)	99.91(39)	1.2	–
[7]	5	bournonite		13.67(15)	n.d.	44.35(24)	16.98(21)	5.15(11)	20.11(21)	100.26(61)	1.1	–
[8]	4	boulangerite-1		n.d.	0.04(04)	54.04(35)	26.51(30)	0.42(11)	18.93(14)	99.94(07)	1.4	–
[9]	4	boulangerite-2		n.d.	0.05(04)	56.50(26)	22.57(21)	1.87(10)	18.66(02)	99.65(24)	1.2	–
[10]	5	geocronite-1		n.d.	0.09(06)	68.45(31)	9.45(10)	4.57(14)	17.40(11)	99.96(32)	−0.7	–
[11]	3	geocronite-2		n.d.	0.13(13)	67.56(39)	10.69(18)	3.79(06)	17.20(03)	99.37(13)	−0.1	–
[12]	3	geocronite-3		n.d.	0.04(01)	68.24(17)	12.08(25)	2.68(05)	16.89(02)	99.94(04)	1.3	–

Formulae

[1] $Ag_{0.15}Pb_{16.09}Sb_{8.83}As_{6.99}S_{39.95}$
[2] $Ag_{0.12}Pb_{15.95}Sb_{8.44}As_{7.49}S_{40.01}$
[3] $Ag_{0.17}Pb_{16.06}Sb_{9.03}As_{6.86}S_{39.92}$
[4] $Cu_{1.07}Ag_{2.70}Pb_{19.69}Sb_{15.08}As_{8.63}S_{56.09}$
[5] $Cu_{1.23}Ag_{2.61}Pb_{19.65}Sb_{15.47}As_{8.00}S_{56.02}$
[6] $Cu_{1.01}Ag_{2.73}Pb_{19.70}Sb_{14.94}As_{8.48}S_{56.12}$
[7] $Cu_{1.02}Pb_{1.02}Sb_{0.66}As_{0.33}S_{2.98}$
[8] $Ag_{0.01}Pb_{4.85}Sb_{4.05}As_{0.10}S_{10.97}$
[9] $Ag_{0.01}Pb_{5.12}Sb_{3.48}As_{0.47}S_{10.92}$
[10] $Ag_{0.05}Pb_{14.03}Sb_{3.29}As_{2.59}S_{23.03}$
[11] $Ag_{0.06}Pb_{13.98}Sb_{3.76}As_{2.17}S_{22.99}$
[12] $Ag_{0.02}Pb_{14.29}Sb_{4.30}As_{1.55}S_{22.82}$

The data are expressed in wt.%. *Number of analyses. [$]chemistry of an untwinned crystal used for single-crystal X-ray diffraction. n.d. – not detected. [#]Charge balance as (Σ(val+)−Σ(val–)) using at.%. [§]N_{calc} is described in the text. Formulae are calculated on the basis of $\Sigma(Me + S) = 72$ atoms per formula unit for veenite, 103 for sterryite, 6 for bournonite, 20 for boulangerite and 43 for geocronite.

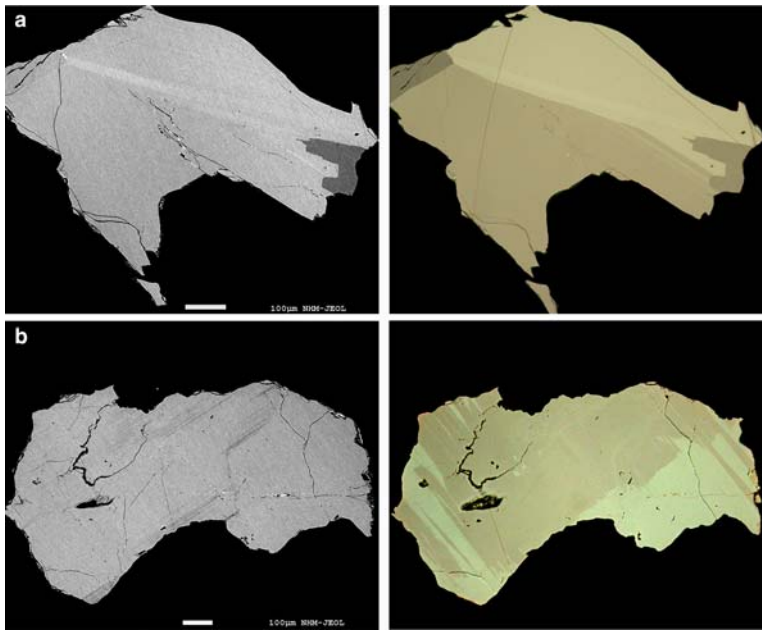


FIG. 1. Polished fragments of veenite in BSE images and corresponding optical images (crossed polars; rare twin lamellae). The dark area in Fig. 1a is sterryite. Lighter and darker varieties of veenite in BSE images are dealt with in the text. Scale bar = 100 μm.

Table 1. Chemical data for associated minerals are not discussed in detail here, being the subject of another publication.

The most interesting aspect of this assemblage is the distribution of As and Sb among the individual phases of this association, in relation to their structure type. Silver concentrates heavily in sterryite whereas it is barely detectable in geocronite and is at the limit of detection in boulangerite. The veenite investigated is not entirely free of silver, although the silver content is very low (0.16–0.18 wt.%), and is copper free.

Incorporation of antimony in veenite exceeds that of arsenic (Table 1). The molar Sb/As ratio varies from 1.13 to 1.32. Three averaged analyses of veenite in Table 1 were processed using the calculation procedures of the homologous order (N) in the sartorite homologous series to which veenite belongs, and molar percentage of Ag-(As,Sb) substituted end-member (Makovicky and Topa, 2015). They are in agreement with the crystal structure determination. The calculated N value varies from 4.04 to 4.08 (the structural value is 4.0) and the molar percentage of the Ag-(As,Sb) substituted end-member is from 2.89 mol.% to 3.98 mol.%, i.e. very low. Atomic ratios in Table 1 are given for veenite, in terms of experimental N values, as $Me_{8N}S_{8N+8}$. The bulk veenite composition, represented by medium grey areas in the back-scatter electron (BSE) images (Fig. 1*a* and 1*b*) is $Ag_{0.15}Pb_{16.09}Sb_{8.83}As_{6.99}S_{39.95}$. This corresponds to N = 4.08 and the percentage of the Ag-(As,Sb) substituted end-member equal to 3.51 mol.%. The bright lamella in the BSE image Fig. 1*a* has composition $Ag_{0.17}Pb_{16.06}Sb_{9.03}As_{6.86}S_{39.92}$ (N = 4.07; 3.98 mol.% of the Ag-(As,Sb) substituted end-member) whereas the dark lamellae typified by those seen in Fig. 1*b* have composition $Ag_{0.12}Pb_{15.95}Sb_{8.44}As_{7.49}S_{40.01}$ (N = 4.04; 2.89 mol.% of the Ag-(As,Sb) substituted end-member).

The average Sb/As ratio is 1.233, much lower than Jambor's (1967) and Jambor's *et al.* (1982) ratio of 1.67, which was based on a combination of electron microprobe data and classical analyses (for some of which he quotes unresolved problems).

Crystal structure

In the present study, the crystal structure of veenite was refined in the space group $P2_1$, with the unit cell parameters $a = 8.4291(15)$, $b = 26.0691(45)$,

https://doi.org/10.1180/minmag.2016.080.141 Published online by Cambridge University Press

TABLE 2. Crystal data and summary of parameters describing data collection and refinement for veenite.

Crystal data	
Chemical formula	$Ag_{0.15}Pb_{16.09}As_{6.99}Sb_{8.83}S_{39.95}$
Formula weight	6217.6
Crystal system	Monoclinic
Space group	$P2_1$ (#4)
D_x (mg m^{-3})	5.91
No. of reflections for cell param.	3665
μ (mm^{-1})	46.3
Unit-cell parameters	a = 8.429(2) Å b = 26.069(5) Å c = 8.962(2) Å β = 117.447(2)°
V (Å^3)	1747.6(18)
Z	1
Crystal form	irregular
Crystal colour	grey metallic
Crystal size (mm)	0.095 × 0.07 × 0.05
Data collection	
T_{min}, T_{max}	0.214, 0.911
No. of measured reflections	14,913
No. of independent reflections	4973
No. of observed reflections	3897
Criterion for observed reflections	$I > 2\sigma(I)$
R_{int} (%), $R_{(sigma)}$(%)	9.01, 7.44
θ_{max}(°)	23.3
Range of *h, k, l*	$-9 \le h \le 9$, $-28 \le k \le 28$, $-9 \le l \le 9$
Refinement	
Refinement on F_o^2	
$R[F_o > 4\sigma(F_o)]$ (%)	3.96
$wR(F_o^2)$ (%)	8.22
S (Goof)	0.951
No. of reflections used in refinement	4973
No. of parameters refined	349
Weighting scheme	a = 0.0229, b = 0 where $P = (F_o^2 + 2F_c^2)/3$
$(\Delta/\sigma)_{max}$	0.002
$\Delta\rho_{max}$ (e/Å^3)	1.49 (0.86 Å from Sb11)
$\Delta\rho_{min}$ (e/Å^3)	–1.95 (0.89 Å from Sb12)
Extinction coefficient	none
Source of atomic scattering factors	*International Tables for X-Ray Crystallography* (1992, Vol. C, Tables 4.2.6.8 and 6.1.1.4)

c = 8.9618(16) Å, β = 117.447(2)°. In this it differs from dufrénoysite, which has a β value of ~90.5°.

The cell parameters and structure-refinement data were obtained using a Bruker AXS three-circle diffractometer equipped with a CCD area detector installed at the University of Salzburg. The *SMART* (Bruker AXS, 1998*a*) system of programs was used for unit-cell determination and data collection, *SAINT+* (Bruker AXS, 1998*b*) for the reduction of the intensity data, and *XPREP* (Bruker AXS, 1997) for space-group determination and empirical absorption correction based on pseudo ψ-scans. The non-centrosymmetric space group $P2_1$ proposed by the *XPREP* program for veenite was chosen. It is consistent with the monoclinic symmetry of the lattice and intensity statistics. An untwinned fragment of veenite was selected, as confirmed by the results of structure refinement (cation occupancies and interatomic distances for cations in the 8 Å cell). The crystal structure of veenite was solved by direct methods (Sheldrick, 2008), which revealed most of the atom positions. In subsequent cycles of the refinement (Sheldrick, 2008), remaining atom positions were deduced from difference-Fourier syntheses by selecting from among the strongest maxima at appropriate distances. The final agreement factors are R_1 = 0.0396 for 3897 reflections with $F_o > 4\sigma(F_o)$ and 0.0822 for all 4973 data. Complete experimental and refinement data for veenite are collected in Table 2. Calculated powder diffraction data are given in Table 3. Atomic position parameters, refined occupancies and U_{eq} parameters are listed in Table 4, whereas a table of complete anisotropic displacement parameters (Table 4*b*) has been deposited with the Principal Editor of *Mineralogical Magazine* at http://www.minersoc.org/pages/e_journals/dep_mat.htm and is also available upon request from the authors. The bond distances are presented in Table 5.

The crystal structure analysis indicated an Sb/As ratio equal to 1.61, similar to that obtained by Jambor *et al.* (1982), whereas our electron microprobe analyses varied between 1.13 and 1.32. With a refinement which includes eight mixed cation sites (Sb involved in two very different types of substitution) and only three compositionally relevant unmixed cation sites (one still showing signs of splitting), and a mixture of split mixed sites and non-split mixed sites, introduced as the development of the refinement dictated, plus the compositional non-homogeneity of the veenite sample, this difference should not be overvalued.

In the [100] projection, the structure follows the structural scheme of the N = 4 member of the

https://doi.org/10.1180/minmag.2016.080.141 Published online by Cambridge University Press

TABLE 3. Calculated powder X-ray diffraction data for veenite.*

$I_{rel.}$	d/Å	h	k	l	$I_{rel.}$	d/Å	h	k	l	$I_{rel.}$	d/Å	h	k	l
25	7.59	0	1	3	29	2.8166	2	6	3	3	1.9279	2	10	6
11	6.77	0	2	3	**73**	**2.7382**	**$\bar{2}$**	**3**	**6**	15	1.9163	$\bar{2}$	7	9
4	6.03	1	3	0	3	2.7056	0	9	3	17	1.9161	2	7	9
15	5.84	0	3	3	4	2.6370	$\bar{2}$	4	6	5	1.8962	0	12	6
2	5.27	$\bar{1}$	2	3	4	2.6366	2	4	6	14	1.8666	$\bar{2}$	12	3
19	5.02	0	4	3	9	2.6326	0	1	9	13	1.8665	2	12	3
2	5.02	$\bar{1}$	4	1	4	2.6307	$\bar{3}$	1	3	5	1.8501	0	14	0
3	4.41	1	5	0	9	2.5928	0	2	9	7	1.8422	$\bar{2}$	8	9
27	4.34	0	5	3	9	2.4624	0	10	3	6	1.8420	2	8	9
2	4.34	$\bar{1}$	5	1	4	2.4497	0	4	9	9	1.8398	$\bar{4}$	2	6
6	4.32	0	6	0	**79**	**2.3752**	**2**	**9**	**0**	10	1.8395	4	2	6
53	4.15	2	1	0	14	2.3300	0	9	6	6	1.8394	$\bar{4}$	6	3
2	4.09	$\bar{1}$	1	5	2	2.2760	2	7	6	7	1.8393	4	6	3
8	3.970	0	0	6	7	2.2756	$\bar{2}$	9	3	20	1.8248	$\bar{2}$	11	6
21	3.924	0	1	6	7	2.2755	2	9	3	20	1.8246	2	11	6
2	3.856	1	5	3	6	2.2574	0	11	3	3	1.8168	4	3	6
4	3.841	1	6	0	14	2.2561	0	6	9	18	1.8018	0	14	3
100	**3.795**	**0**	**2**	**6**	37	2.2318	$\bar{2}$	1	9	3	1.8006	2	13	0
73	3.792	0	6	3	41	2.2314	2	1	9	3	1.7908	$\bar{2}$	1	12
2	3.782	2	3	0	11	2.1692	0	10	6	4	1.7906	2	1	12
18	3.607	0	3	6	3	2.1683	$\bar{2}$	3	9	6	1.7807	0	13	6
3	3.590	1	0	6	4	2.1680	2	3	9	9	1.7781	$\bar{2}$	2	12
32	3.573	$\bar{2}$	2	3	2	2.1549	$\bar{2}$	8	6	8	1.7779	2	2	12
36	3.572	2	2	3	2	2.1547	2	8	6	3	1.7677	$\bar{2}$	9	9
58	3.414	$\bar{2}$	3	3	12	2.1525	0	7	9	3	1.7676	2	9	9
60	3.414	2	3	3	11	2.1251	$\bar{2}$	10	3	17	1.7638	4	8	0
4	3.384	0	4	6	12	2.1250	2	10	3	6	1.7494	$\bar{4}$	5	6
3	3.354	0	7	3	**64**	**2.1033**	**4**	**0**	**0**	6	1.7492	4	5	6
2	3.315	$\bar{1}$	3	6	3	2.0828	0	12	3	3	1.7218	$\bar{4}$	8	3
12	3.265	2	5	0	2	2.0682	4	2	1	3	1.7217	4	8	3
69	**3.238**	**0**	**8**	**0**	2	2.0561	$\bar{2}$	5	9	9	1.7071	$\bar{4}$	6	6
45	3.224	$\bar{2}$	4	3	2	2.0558	2	5	9	10	1.7069	4	6	6
44	3.223	2	4	3	6	2.0546	2	11	0	3	1.6962	$\bar{2}$	5	12
56	3.151	0	5	6	24	2.0490	0	8	9	4	1.6959	2	5	12
86	3.020	$\bar{2}$	5	3	2	2.0381	2	9	6	4	1.6873	0	15	3
87	**3.020**	**2**	**5**	**3**	3	1.9883	$\bar{2}$	6	9	2	1.6609	$\bar{4}$	7	6
26	2.9979	0	8	3	3	1.9881	2	6	9	2	1.6607	4	7	6
82	**2.9220**	**0**	**6**	**6**	2	1.9848	0	0	12	5	1.6575	$\bar{2}$	6	12
13	2.8873	$\bar{2}$	0	6	6	1.9618	0	2	12	5	1.6573	2	6	12
10	2.8868	2	0	6	12	1.9480	0	9	9	2	1.5760	0	2	15
4	2.8695	$\bar{2}$	1	6	2	1.9398	$\bar{4}$	4	3	3	1.5754	0	10	12
4	2.8690	2	1	6	3	1.9397	4	4	3	9	1.5616	0	3	15
17	2.8181	$\bar{2}$	2	6	20	1.9343	0	3	12	3	1.5613	$\bar{4}$	9	6
15	2.8176	2	2	6	4	1.9325	0	13	3	10	1.5421	0	4	15

*The theoretical pattern was calculated with *PowderCell 2.3* software (Kraus and Nolze, 1999) in Debye-Scherrer configuration employing Cu$K\alpha$ radiation ($\lambda = 1.540598$ Å), a fixed slit, and no anomalous dispersion, for $I_{rel} > 1.99$. Cell parameters, space group, atom positions, site occupancy factors and isotropic displacement factors from the crystal structure determination were used. The strongest lines are given in bold.

sartorite homologous series. It was refined with 4 pure Pb sites, 6 mixed (Pb,Sb) sites, two As sites, two Sb sites and two mixed (As,Sb) sites (Table 4). As much as possible, the sites were named in agreement with the structure description of structurally related dufrénoysite by Ribar *et al.* (1969).

https://doi.org/10.1180/minmag.2016.080.141 Published online by Cambridge University Press

TABLE 4. Coordinates, site occupancy factors (s.o.f.) and displacement parameters of atoms in veenite. A table of complete anisotropic displacement parameters (Table 4*b*) has been deposited at http://www.minersoc.org/pages/e_journals/dep_mat.htm

Ribar*	Label	s.o.f.	*x*	*y*	*z*	$U_{(eq)}$
Pb1	Pb1	1	0.36300(17)	0.19117(5)	0.97388(16)	0.0394(4)
Pb2	Pb2	1	0.85929(17)	0.19444(5)	0.96302(16)	0.0400(4)
Pb3	Pb3	1	0.11436(16)	0.28789(5)	0.46217(16)	0.0376(3)
Pb4	Pb4	1	0.61162(16)	0.28496(5)	0.47421(16)	0.0385(3)
Pb5	Pb5/Sb9	0.954(10)/0.046	0.77923(17)	0.41873(5)	0.79527(17)	0.0353(5)
Pb6	Pb6/Sb10	0.865(10)/0.135	0.52608(16)	0.06244(5)	0.29870(17)	0.0310(5)
Pb7	Pb7	0.511(10)	0.8182(11)	0.4394(3)	0.3498(9)	0.0354(12)
	Sb11	0.489(10)	0.814(2)	0.4434(6)	0.3864(16)	0.0354(12)
Pb8	Pb8/Sb12	0.718(10)/0.282	0.27500(18)	0.42329(5)	0.79468(18)	0.0332(5)
As1	As1	0.509(18)	0.164(5)	0.3346(11)	0.015(3)	0.044(2)
	Sb1	0.491(18)	0.169(3)	0.3431(7)	0.047(2)	0.044(2)
As2	As2	1	0.6551(3)	0.32811(11)	0.0534(3)	0.0185(7)
As3	As3	1	0.3916(4)	0.15066(11)	0.5304(3)	0.0194(6)
As4	Sb4	1	0.9088(3)	0.14823(8)	0.5391(2)	0.0334(5)
As5	Sb5	0.516(9)	0.5670(19)	0.0410(6)	0.8912(15)	0.0233(12)
	Pb9	0.484(9)	0.5614(11)	0.0410(3)	0.8526(9)	0.0233(12)
As6	As6	0.538(15)	0.071(2)	0.0548(7)	0.862(3)	0.0041(18)
	Sb6	0.462(15)	0.0437(18)	0.0439(5)	0.8605(19)	0.0041(18)
As7	Sb7	0.485(10)	0.036(3)	0.0530(9)	0.306(3)	0.0307(12)
	Pb10	0.515(10)	0.0247(14)	0.0594(5)	0.3041(15)	0.0307(12)
As8	Sb8	1	0.3046(3)	0.43630(10)	0.3590(3)	0.0407(6)
	S1	1	0.4883(9)	0.2129(3)	0.7195(9)	0.0284(18)
	S2	1	0.2313(8)	0.2682(3)	0.2011(8)	0.0188(16)
	S3	1	0.7795(7)	0.3054(3)	0.8865(7)	0.0215(14)
	S4	1	0.4288(8)	0.3802(3)	0.5916(8)	0.0180(15)
	S5	1	0.4436(7)	0.3903(3)	0.2162(7)	0.0258(15)
	S6	1	0.1220(8)	0.4943(3)	0.5403(8)	0.0207(15)
	S7	1	0.6775(8)	0.4967(3)	0.5506(9)	0.0252(17)
	S8	1	0.5733(8)	0.4877(3)	0.9434(9)	0.0237(16)
	S9	1	0.1149(9)	0.4925(3)	0.9495(9)	0.0227(15)
	S10	1	0.1805(8)	0.1033(3)	0.1015(8)	0.0231(17)
	S11	1	0.5278(7)	0.1770(2)	0.3789(7)	0.0174(13)
	S12	1	0.7841(7)	0.0990(2)	0.7314(7)	0.0219(14)
	S13	1	0.2003(7)	0.0989(2)	0.7261(7)	0.0187(13)
	S14	1	0.9804(9)	0.2262(3)	0.7056(8)	0.0219(16)
	S15	1	0.7431(8)	0.2600(3)	0.2266(8)	0.0187(15)
	S16	1	0.3622(7)	0.3050(2)	0.8886(7)	0.0177(13)
	S17	1	0.9117(8)	0.3707(3)	0.5851(9)	0.0199(15)
	S18	1	0.0309(7)	0.3904(2)	0.2250(7)	0.0210(14)
	S19	1	0.6623(8)	0.1135(3)	0.0925(8)	0.0203(16)
	S20	1	0.1065(7)	0.1804(3)	0.3805(7)	0.0212(14)

*Site nomenclature in dufrénoysite (Ribar *et al.*, 1969).

Both the coordination polyhedra with spatially separated component atoms (complicating the atom designation), and those which had to be refined with one set of positional coordinates, were encountered. The pure Pb sites form two alternating columns of trigonal coordination prisms, the Pb1–Pb2 column, and the Pb3–Pb4 column, respectively (Fig. 2).

The slabs between adjacent puckered planes of trigonal coordination prisms of Pb are a modified (301) slice of the archetypal structure of SnS. They consist of parallel ribbon-like fragments of tightly

https://doi.org/10.1180/minmag.2016.080.141 Published online by Cambridge University Press

https://doi.org/10.1180/minmag.2016.080.141 Published online by Cambridge University Press

TABLE 5. Selected interatomic distances (Å) in veenite.

Pb1-		Pb2-		Pb3-		Pb4-		Pb5/Sb9–		Pb6/Sb10-	
S1	2.975(10)	S1	2.912(6)	S20	2.889(8)	S11	2.931(5)	S7	2.818(8)	S8	2.744(8)
S19	3.020(7)	S3	2.977(8)	S15	2.948(6)	S15	2.974(9)	S4	2.845(6)	S10	2.828(6)
S16	3.064(6)	S14	3.037(9)	S2	2.972(9)	S2	3.037(5)	S17	2.881(9)	S19	2.909(8)
S13	3.129(5)	S12	3.113(6)	S17	3.245(9)	S17	3.172(7)	S3	3.065(8)	S11	3.070(6)
S14	3.141(6)	S19	3.214(8)	S18	3.283(6)	S14	3.220(7)	S9	3.164(7)	S7	3.137(9)
S10	3.247(8)	S20	3.360(5)	S14	3.300(9)	S3	3.334(6)	S8	3.183(9)	S6	3.177(7)
S11	3.255(6)	S10	3.379(7)	S4	3.366(7)	S4	3.338(8)	S18	3.514(5)	S12	3.592(5)
S2	3.390(8)	S15	3.405(8)	S16	3.436(5)	S1	3.398(9)				
S15	3.453(6)	S2	3.452(6)	S1	3.518(7)	S5	3.446(7)				
Pb7-		Sb11-		Pb8/Sb12-		As1-		Sb1-		As2-	
S17	2.597(11)	S17	2.468(16)	S6	2.753(7)	S2	2.286(29)	S2	2.308(19)	S15	2.247(8)
S6	2.737(10)	S7	2.642(20)	S8	2.798(7)	S16	2.533(43)	S5	2.436(20)	S3	2.266(8)
S18	2.819(12)	S6	2.665(16)	S4	2.903(9)	S5	2.645(30)	S18	2.671(25)	S16	2.297(5)
S7	2.974(13)	S5	3.098(16)	S9	2.954(9)	S18	2.977(39)	S16	2.790(27)	S5	3.215(8)
S5	3.091(10)	S18	3.128(20)	S17	3.079(6)	S3	2.995(39)	S3	3.076(23)		3.247(6)
S8	3.490(10)	S8	3.713(15)	S16	3.192(5)						
				S5	3.476(6)						
As3-		Sb4-		Sb5-		Pb9-		As6		Sb6-	
S1	2.213(8)	S14	2.427(8)	S19	2.477(16)	S19	2.689(11)	S13	2.284(26)	S12	2.420(14)
S11	2.252(8)	S13	2.589(5)	S8	2.673(19)	S9	2.780(10)	S10	2.287(24)	S10	2.469(16)
S20	2.281(6)	S12	2.719(7)	S9	2.701(16)	S8	2.911(13)	S12	2.437(16)	S13	2.591(19)
S13	3.179(8)	S20	2.772(8)	S13	3.131(15)	S12	2.978(12)	S8	3.205(17)	S9	2.929(21)
S12	3.242(6)	S11	2.947(6)	S12	3.178(19)	S13	3.106(10)	S9	3.223(27)	S8	3.229(14)
		S19	3.673(6)	S7	3.706(14)	S7	3.426(10)			S6	3.450(17)
						S5	3.974(11)				
Sb7-		Pb10-		Sb8-							
S9	2.581(24)	S9	2.669(14)	S4	2.360(7)						
S7	2.603(23)	S7	2.767(13)	S18	2.375(6)						
S6	2.776(30)	S6	2.818(17)	S5	2.415(8)						
S10	2.936(31)	S10	2.920(17)	S6	3.098(9)						
S19	3.243(22)	S19	3.095(12)	S7	3.214(7)						
S20	3.386(25)	S20	3.234(15)	S9	3.572(8)						
S13	3.566(26)	S13	3.520(14)								

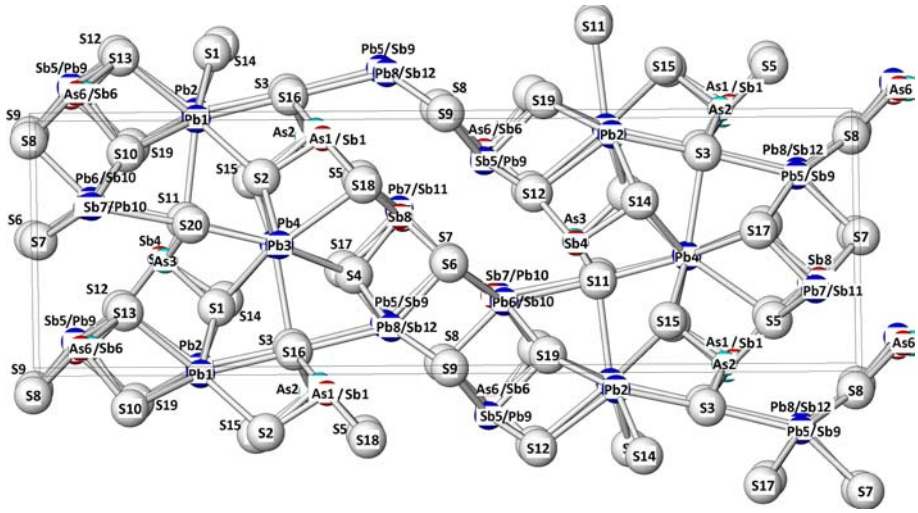


FIG. 2. The crystal structure of veenite from Madoc in oblique projection approximately along [100]. Pb: dark blue; Sb: red; As: light blue; and S: white.

bonded double-layers, separated by interspaces which accommodate lone electron pairs of As, Sb, and also those of Pb (Fig. 2).

On the opposing surfaces of each double-layer segment, antimony and arsenic form similar configurations (Fig. 3). The marginal, side-oriented AsS_3 groups of the segment As2 and As3, respectively, on the two surfaces, join with mixed-occupancy (As,Sb) groups, or with Sb, both with a split and flipping coordination (with different sets of short bonds). These are followed by Sb or (As,Sb) groups attached to the latter. Together they form short crankshaft fragments Me_3S_7. When we do not consider different distributions of Sb and mixed cation positions over such a chain, the configurations on the opposite side and opposite margins of the double-ribbon nearly correspond to one another; they are antiparallel and related by an inversion centre. On one surface, these crankshaft fragments Me_3S_7 are composed of As2 positioned at the margins (Fig. 3), a mixed As1 & Sb1 site, and the Sb8 position (this one unevenly flipping and with *Me–S* distances which might indicate a small admixture of As; Table 5). On the opposing surface, marginally positioned As3 is followed by Sb4 with an evenly flipping character and the chain fragment is terminated by a mixed As6–Sb6 site which has a clear three-fold bonding coordination for both components.

There is no unbiased way of placing (and even 'refining') the trace amount of 0.15 Ag per formula unit in this complex structure. In polloneite (Topa *et al.*, 2017), silver mixes with Sb/As in the sites which correspond to our flipping As1 & Sb1 and Sb4 sites.

In the median portions of the double-layer segments, one of the double-layer surfaces hosts configurations $(Sb,Pb)_2S_4$ with 'paired-cations': the coordination polyhedra of these cations are connected by shorter *Me*–S bonds (these are averages of the Sb–S and Pb–S distances) to two common sulfur atoms. These positions are labelled as the split Pb7–Sb11 and Pb10–Sb7 sites (Fig. 3), with occupancies refined as nearly 50:50, with a minute surplus of Pb (Table 4). Shifted by ~2 Å along [100], and connected by one of the shorter bonds to the latter assemblage, is the sole mixed Sb5–Pb9 (~50:50) position on the opposite surface, whereas the analogue of the other (Sb,Pb) site from the $(Sb,Pb)_2S_4$ group is a Pb-rich Pb8 position with typical bond distances of Pb (Table 5, Fig. 3). The pattern of short and long bond distances on the surface of a double-layer is well organized, with the above configurations distributed in a sort of a chessboard scheme, so that the layer avoids stresses and strains (Fig. 3).

Comparisons with related sulfosalts

In the cation distribution and polyhedron scheme, the double-layer of veenite resembles the 'R2' double-layer segment from the crystal structure of polloneite (Figs 4 and 6). The principal difference is in the positions (Sb,As)1 (that follows after the

https://doi.org/10.1180/minmag.2016.080.141 Published online by Cambridge University Press

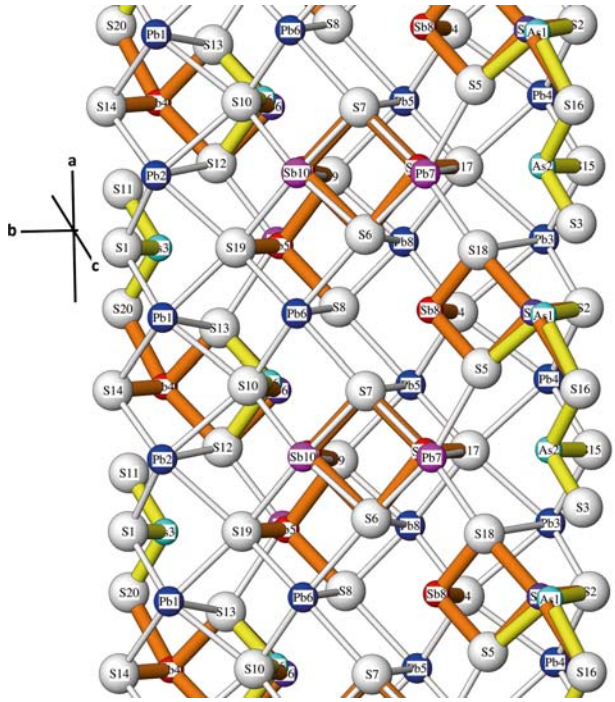


FIG. 3. A tightly-bonded double-layer ribbon from the veenite structure. Red spheres and orange bonds: Sb; light-blue atoms and yellow bonds: As; purple spheres: partly substituted Pb; dark-blue spheres with white bonds: full Pb. For unabbreviated atom labels of mixed sites see Fig. 2 and Table 4.

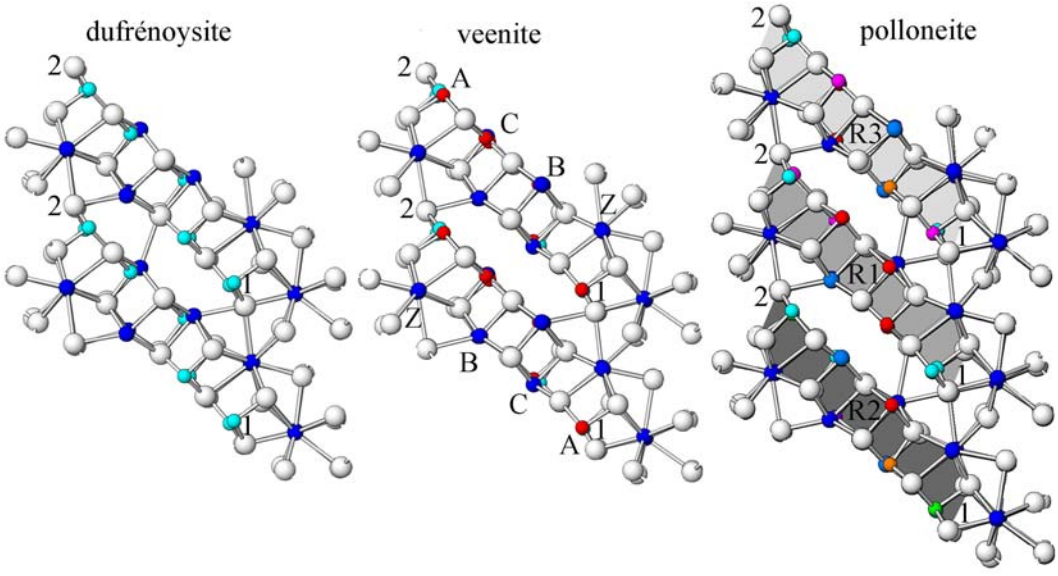


FIG. 4. Portions of the crystal structures of dufrénoysite, veenite and polloneite projected along the 8.4 Å direction. For colour scheme see Figs 2 and 3. Cation columns in the structures are denoted as the Z, A, B and C columns according to the scheme proposed by Berlepsch *et al.* (2001).

https://doi.org/10.1180/minmag.2016.080.141 Published online by Cambridge University Press

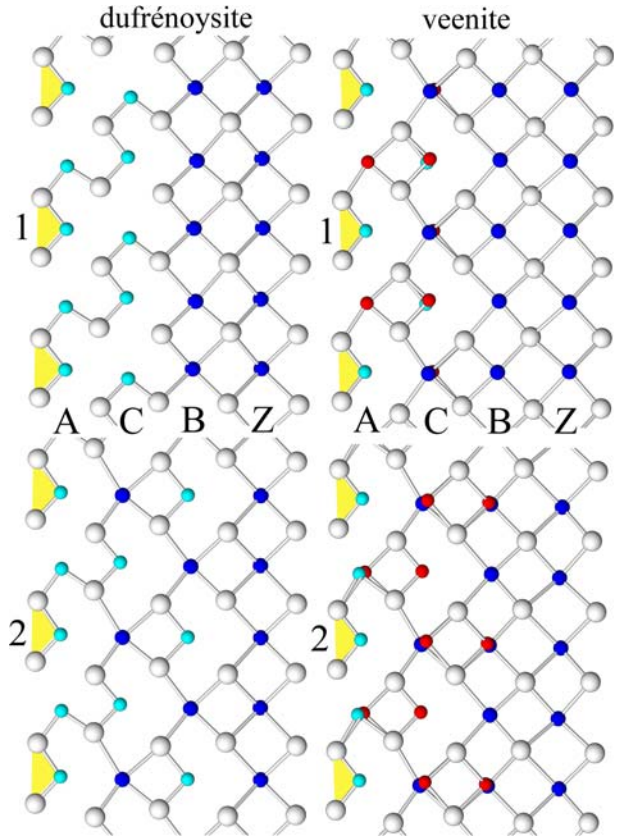


FIG. 5. Cation configurations on the two different surfaces of tightly-bonded double layers in the structures of dufrénoysite (*left*) and veenite (*right*). For conventions see Fig. 4.

marginal pyramid of As2) and Sb4 (that follows after the similarly positioned As3 pyramid), which (especially Sb1) are split-and-flipping positions in veenite, situated asymmetrically in their respective polyhedron, similar to the situation observed in barikaite in which flipping is of lesser importance (Makovicky and Topa, 2013). This is to be compared with the symmetrically positioned and coordinated (Ag, Sb) positions in the 'R2' double-layer type in polloneite (Topa *et al.*, 2017). The 'R1' and 'R3' layer types in polloneite lack the split and flipping character (Topa *et al.*, 2017).

Veenite, polloneite, dufrénoysite and barikaite (all of which are N = 4 homologues of sartorite; Table 6) can be compared using plots of cation-anion populated surface layers of the double-layer segments from their structures (Figs 4–6). For these comparisons, we have to name the four columns of polyhedra in one N = 4 segment, which are parallel to the 8.4 Å period, and, respectively, form one of the two surfaces of this tightly-bonded segment. We shall use the nomenclature of Berlepsch *et al.* (2001): the marginal column of trigonal coordination prisms occupied by Pb is designated a Z column, the inner column of the segment, situated next to it is the B column, followed by the C column, and by the A column at the opposite margin of the segment; the latter column has coordinations typical for a marginal facies.

The Z column in all the examined structures is occupied by prismatically coordinated Pb. The A column is the anchoring column of crank-shaft chains, in which a side-oriented AsS_3 group alternates with the next polyhedron of the chain – this can be a bottom- (or top-) oriented As (in dufrénoysite), or Sb, or a mixed Sb-As position. The latter sometimes displays a split-flipping character (Figs 4–6). It is a mixed As,Sb site in polloneite. In all these structures, the crankshaft chain continues into the adjacent C column, either

https://doi.org/10.1180/minmag.2016.080.141 Published online by Cambridge University Press

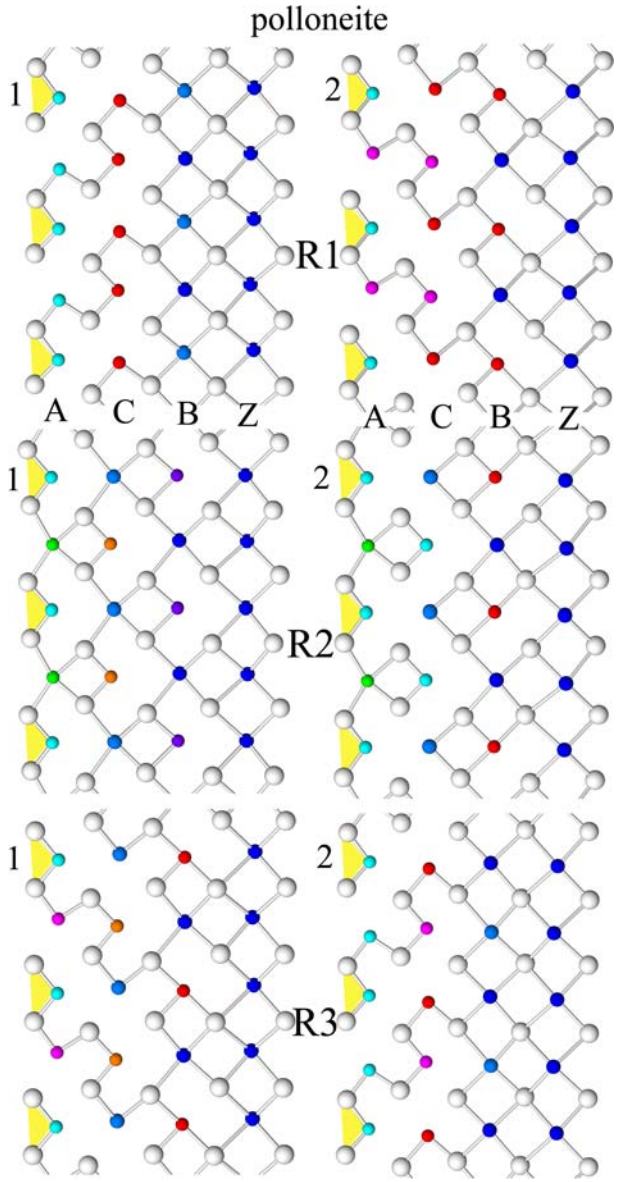


FIG. 6. Cation configurations on the two different surfaces of tightly-bonded R1, R2 and R3 double layers in the structure of polloneite, (*upper*), (*middle*) and (*lower*) respectively. For conventions see Fig. 5; Ag: green; mixed site: orange.

as a side-bonded As (dufrénoysite, veenite in part and polloneite) or as an Sb (resp. Sb/As) site (veenite, in part). The alternating position in this column varies: it is a bottom/top bonded Sb site or a Pb site, as observed in polloneite, or a top-bonded As position in one layer type in dufrénoysite, corresponding to the '0.80Pb site' in the opposing surface of a double-layer in this structure (Ribar *et al.*, 1969); we interpret the latter site as a mixed (Pb, As) site in veenite and not as a partly vacant Pb site. Furthermore, it is an evenly flipping Sb site in barikaite, and mixed (Pb,Sb) sites in veenite. The latter site pairs with (Pb,Sb), or with Pb, from the B columns of the veenite structure. The just mentioned Pb and (Pb,Sb) sites are not a continuation of the crankshaft chain from the A–C set.

https://doi.org/10.1180/minmag.2016.080.141 Published online by Cambridge University Press

TABLE 6. Comparative data for veenite and related sartorite homologues with N = 4.

Mineral	Veenite	Polloneite	Dufrénoysite	Rathite	Carducciite	Barikaite
Formula	$Pb_{16}Sb_9As_7S_{40}$	$AgPb_{46}As_{26}Sb_{23}S_{120}$	$Pb_{16}As_{16}S_{40}$	$Ag_2Pb_{9.5}Tl_{1.5}As_{18}SbS_{40}$	$Ag_2Pb_{12}As_{10}Sb_8S_{40}$	$Ag_{\sim 3}Pb_{10}As_{11}Sb_8S_{40}$
Crystal system	monoclinic	monoclinic	monoclinic	monoclinic	monoclinic	monoclinic
Space group	$P2_1$	$P2_1$	$P2_1$	$P2_1/c$	$P2_1/c$	$P2_1/c$
Cell parameters (Å)						
a	8.429(2)	8.413(2)	8.47(4)	8.496(1)	8.4909(3)	8.53
b	26.069(5)	25.901(5)	25.74(4)	7.969(1)	8.0227(3)	8.08
c	8.962(2)	23.817(5)	7.90(1)	25.122(3)	25.3957(9)	24.95
β(°)	117.447(2)	90.01(3)	90.35(12)	100.704(2)	100.382(2)	100.66
Z	1	1	1	1	1	1
Ref.*	[1]	[2]	[3]	[4]	[5]	[6]

*[1]: this study; [2]: Topa *et al.* (2017); [3]: Ribar *et al.* (1969); [4]: Berlepsch *et al.* (2002); [5]: Biagioni *et al.* (2014); [6]: Topa *et al.* (2013).
#Transformed from: $P2_1/n$, $a = 8.533(1)$, $b = 8.075(1)$, $c = 24.828(2)$ and $\beta = 99.077(1)$.

The B column is at least 50% occupied by Pb in all the mentioned structures (they are Pb-rich phases), with the exception of barikaite because this mineral is the only substantially Ag-Sb substituted member of the series examined here; we include it in these considerations because of its mixed Sb-As character. In dufrénoysite, Pb alternates with side-bonded As on one surface, and with '0.8Pb' in on the opposite surface, whereas in veenite a pure Pb-occupied B column coexists with a B column on the opposing surface, in which Pb alternates with (Pb,Sb) in about equal amounts. In polloneite, each set of double-layer segments has an alternation of Pb with flipping Sb on one side and is Pb-occupied (resp. (Pb,Sb) alternating with Pb) on the other side of the double-layer. In barikaite, alternation of a $Pb_{0.4}Ag_{0.3}Sb_{0.3}$ position with an $Ag_{50}Sb_{50}$ site takes place in the B column (Makovicky and Topa, 2013). This fairly confusing picture is easily resolved by visual inspection of Figs 5, 6 and 7.

Crank-shaft chains are best defined for dufrénoysite, as 3- and 4-member chains (when one mixed Pb,As site is included, even as 5-member chains). They are perpendicular to one another across the tightly-bonded double-layer. In veenite, introduction of Sb breaks down the chain pattern, leaving only rudimentary 3-member chains and a cation pair (as described above). These chains are antiparallel on the two surfaces. In polloneite, in one, 'R2' type of double layers (Topa *et al.*, 2017), the chain pattern is replaced entirely by finite groups, in the others they largely correspond to those in dufrénoysite, with occasional Pb or a flipping Sb position introduced. They are perpendicular to one another inside these R1 and R3 type double layers (Topa *et al.*, 2017). The 4-to-6 member distorted chains with flipping sites and an (Ag,Sb) site in barikaite are antiparallel, in a manner similar to rathite (Berlepsch *et al.*, 2002).

The antiparallelity of (although rudimentary) crankshaft chains in the double-layer segments of veenite is unique for such a Pb-rich phase, and is very different from dufrénoysite in which the well-developed crankshaft chains are perpendicular to one another. The double-layer in veenite is very close to the R2 double-layer in polloneite; the main difference is the asymmetry of the marginal (As,Sb)1 position in veenite and different percentages of Pb and Sb in the four central positions (two and two of which are paired *via* common sulfur pairs). Thus, the two double-layers are almost identical.

The cation–anion contacts *via* the interspace between adjacent double-layers in veenite proceed

https://doi.org/10.1180/minmag.2016.080.141 Published online by Cambridge University Press

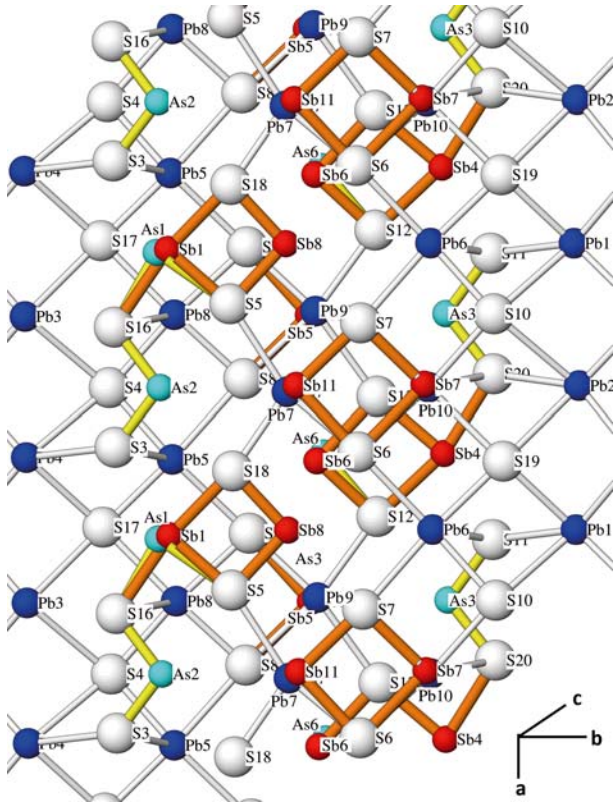


FIG. 7. Interlayer match in the crystal structure of veenite. For conventions see Fig. 3.

via a pseudo-inversion centre situated between Pb7 and Pb9, both being the mixed Pb-Sb sites (Fig. 7). Thus, the chain fragment configurations are not only antiparallel but also inverted. From one double-layer segment to the next one, an identical configuration moves 4.2 Å in the [$\bar{1}$00] direction, which is a cause of the large β angle. The interspace between double-layers in dufrénoysite (Topa and Makovicky, unpublished data) has the facing, (pseudo-) corresponding crankshaft chains perpendicular to one another with a shift of 2.1 Å along the *c* axis in the direction opposite to the shift of 2.1 Å inside the double layer (where the crankshaft chains are perpendicular to one another as well). The resulting β angle is theoretically equal to 90°, as observed.

Implications

The current crystal structure determination on veenite, compared with that on dufrénoysite by Ribar *et al.* (1969) and with further structure determinations on dufrénoysite by us (in prep.) demonstrates that veenite is not just a Sb-rich analogue of dufrénoysite but a mineral species with its own structural architecture, very different from, and not freely miscible with, the arsenic sulfosalt dufrénoysite. It is also another example that attempts to ignore the As:Sb ratios in complex sulfides are contrary to their crystal chemistry and structural principles.

The present data enlarge substantially the description of veenite published by Jambor (1967) and Jambor *et al.* (1982). He described only the 4 Å subcell of veenite, as delineated by a set of strong reflections in single-crystal diffraction photographs: $a = 4.22$ Å, $b = 26.2$ Å, $c = 7.90$ Å, possible orthorhombic space groups $P2_1cn$ or $Pmcn$. The symmetry (and metrics) of the true cell remained unknown. The powder pattern of veenite was found close to that of dufrénoysite but 'contracted in the low-theta region'. It was fully indexed on the basis of the 4.2 Å subcell. No crystallographic information on veenite was given in the re-examination report by Jambor *et al.* (1982).

The 'R1' ribbon of polloneite (Topa *et al.*, 2017) has cation composition $Pb_{6.9}As_{4.49}Sb_{4.61}$, i.e. As ≈

https://doi.org/10.1180/minmag.2016.080.141 Published online by Cambridge University Press

Sb, the 'R2' ribbon has corresponding composition $Pb_{7.61}As_{3.3}(Sb,Ag)_{5.09}$, with Sb > As, and the 'R3' ribbon has the cations $Pb_{7.29}As_{4.96}Sb_{3.75}$, As ≥ Sb; all cases with 16 cation sites. The prominent Sb ≥ As character of the 'R2' ribbon determines its unique configurations and affinity to Ag.

The double-layer ribbon in veenite (the only type in the structure), has cation composition $Pb_{8.05}Sb_{4.91}As_{3.05}$, close to that of the 'R2' ribbon of polloneite, $Pb_{7.61}(Sb,Ag)_{5.09}As_{3.30}$, and far from the other ribbon types in this mineral. Together with the very close principal structural features, this chemical similarity leads to a remarkable model of 'excess' Sb accommodation in polloneite: two double-layer ribbons richer with As, with structural affinity to dufrénoysite, alternate with one ribbon which is enriched in Sb, and is of the veenite structural type.

Acknowledgements

The authors are grateful to Kim Tait, Brendt Hyde and Frank Keutsch who supplied the valuable veenite material; without it this work would not have been possible. Careful reviews by Frantisek Laufek, Peter Leverett, an anonymous reviewer and the Associate Editor Ed Grew are gratefully acknowledged.

References

Biagioni, C., Orlandi, P., Moëlo, Y. and Bindi, L. (2014) Lead-antimony sulfosalts from Tuscany, (Italy). XVI. Carducciite, $(AgSb)Pb_6(As,Sb)_8S_{20}$, a new Sb-rich isotype of rathite from the Pollone mine,Valdicastello Carducci: occurrence and crystal structure. *Mineralogical Magazine*, **78**, 1775–1793.

Berlepsch, P., Makovicky, E. and Balić-Žunić, T. (2001) Crystal chemistry of sartorite homologues and related sulfosalts. *Neues Jahrbuch für Mineralogie, Abhandlungen*, **176**, 45–66.

Berlepsch, P., Armbruster, T. and Topa, D. (2002) Structural and chemical variations in rathite, $Pb_8Pb_{4-x}(Tl_2As_2)_x(Ag_2As_2)As_{16}S_{40}$: modulations of a parent structure. *Zeitschrift für Kristallographie*, **217**, 581–590.

Bruker AXS (1997) *SHELXTL, Version 5.1*. Bruker AXS, Inc., Madison, WI 53719, USA.

Bruker AXS (1998*a*) *SMART, Version 5.0*. Bruker AXS, Inc., Madison, WI 53719, USA.

Bruker AXS (1998*b*) *SAINT, Version 5.0*. Bruker AXS, Inc., Madison, WI 53719, USA.

Jambor, J.L. (1967) New lead sulfantimonides from Madoc, Ontario – Part 1. *Canadian Mineralogist*, **9**, 7–24.

Jambor, J.L., Laflamme, J.H.G. and Walker, D.A. (1982) A re-examination of the Madoc sulfosalts. *Mineral Record*, **13**, 93–100.

Kraus, W. and Nolze, G. (1999) *PowderCell for Windows*, V2.3 – Federal Institute for Material Research and Testing, Berlin, Germany.

Makovicky, E. and Topa, D. (2013) The crystal structure of barikaite. *Mineralogical Magazine*, **77**, 3093–3104.

Makovicky, E. and Topa, D. (2015) Crystal chemical formula for sartorite homologues. *Mineralogical Magazine*, **79**, 25–31.

Ribar, B., Nicca, C. and Nowacki, W. (1969) Dreidimensionale Verfeinerung der Kristallstruktur von Dufrénoysit, $Pb_8As_8S_{20}$. *Zeitschrift für Kristallographie*, **130**, 15–40.

Sheldrick, G.M. (2008) A short history of *SHELX*. *Acta Crystallographica*, **A64**, 112–122.

Topa, D., Makovicky, E., Tajeddin, H., Putz, H. and Zagler, G. (2013) Barikaite, $Ag_3Pb_{10}(Sb_8As_{11})_{\Sigma 19}S_{40}$, a new member of the sartorite homologous series. *Mineralogical Magazine*, **77**, 3039–3046.

Topa, D., Keutsch, F.N., Makovicky, E., Kolitsch, U. and Paar, W. (2017) Polloneite, a new complex Pb(Ag)-As-Sb sulfosalt from the Pollone mine, Apuan alps, Tuscany, Italy. *Mineralogical Magazine*, https://doi.org/10.1180/minmag.2017.081.003.

https://doi.org/10.1180/minmag.2016.080.141 Published online by Cambridge University Press